

Electronic Supplementary Information

Efficient Ambipolar Transport Property in Alternate Stacking Donor-Acceptor Complexes: From Experiment to Theory

Yunke Qin,^{a,c,†} Changli Cheng,^{b,†} Hua Geng,^{a,*} Chao Wang,^{a,c} Wenping Hu,^a Wei Xu,^{a,*} Zhigang Shuai,^{b,*} and Daoben Zhu^{a,*}

^a Beijing National Laboratory for Molecular Sciences, Key Laboratory of Organic Solids, Institute of Chemistry, Chinese Academy of Sciences, Beijing 100190 (P. R. China) E-mail: hgeng@iccas.ac.cn; wxu@iccas.ac.cn; zhudb@iccas.ac.cn

^b Chemistry Department, Tsinghua University, Beijing 100084 (P. R. China) E-mail: zgshuai@tsinghua.edu.cn

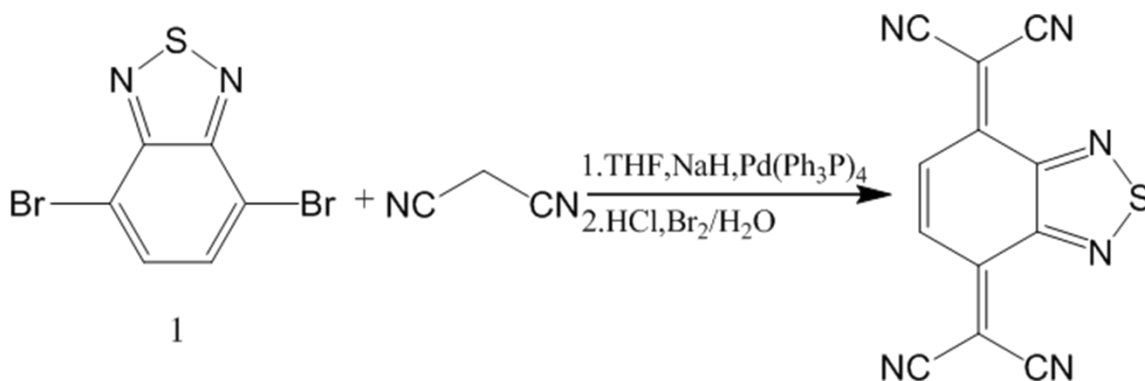
^c University of Chinese Academy of Sciences, Beijing 100049 (P. R. China)

† Y. Qin and C. Cheng contributed equally to this work.

1. Experimental Details

Synthesis of 1,2,5-Thiadiazolotetra-cyanoquinodimethane (SNTCNQ).

The compound SNTCNQ was synthesized via Pd-catalyzed coupling followed by oxidation with saturated Br₂/H₂O. (Scheme S1)



Scheme S1. Synthetic procedure for SNTCNQ.

Under argon atmosphere, to a solution of Malononitrile (0.660 g, 10 mmol) in anhydrous tetrahydrofuran (50 mL) was added sodium hydride (0.24 g, 20 mmol) at ice bath temperature, and the resulting suspension was stirred for 30 min at room temperature. Then tetrakis(triphenylphosphine)palladium (0.174 g, 0.15 mmol) and the precursor 1 (0.294 g, 1 mmol) were added to that suspension. The mixture was heated under reflux for 20 h, and then treated with aqueous hydrochloric acid solution until pH = 1~2. After 30 min, 25 mL of saturated Br₂/H₂O solution was added, and the reaction mixture was stirred about 5 min. Considerable yellow solid precipitated and then filtered. The solid was dissolved in acetone followed by addition of pure water to precipitate the product. Pure yellow product can afford after repeated that procedure several times.

Growth of the self-assembled microcrystal and device fabrication: The SiO₂/Si substrate was heavily doped n-type Si wafer with a 300 nm thick SiO₂ layer and a capacitance of 11 nF•cm⁻². Bare substrates were successively cleaned with pure water, hot concentrated sulfuric acid-hydrogen peroxide solution (H₂SO₄:H₂O₂ = 2:1), pure water and pure isopropanol. Self-assembled co-crystal was conducted by using the drop-casting method. In a typical preparation progress, SiO₂/Si substrate was put into a Peri-dish and saturated solution of complex in chlorobenzene (molar ratio of 1:1) was dropped onto the substrates, until the whole substrate was covered. The solvent was evaporated in the

Peri-dish with a lid at room temperature. Afterwards co-crystals were obtained as described above and samples were annealed at 60°C in vacuum for one hour to get rid of any residues. Consequently drain and source Au electrodes were deposited on the micro-crystal by thermal evaporation using organic ribbon mask method¹ to realize a bottom-gate, top-contact OFET.

2. Additional Characterization Data

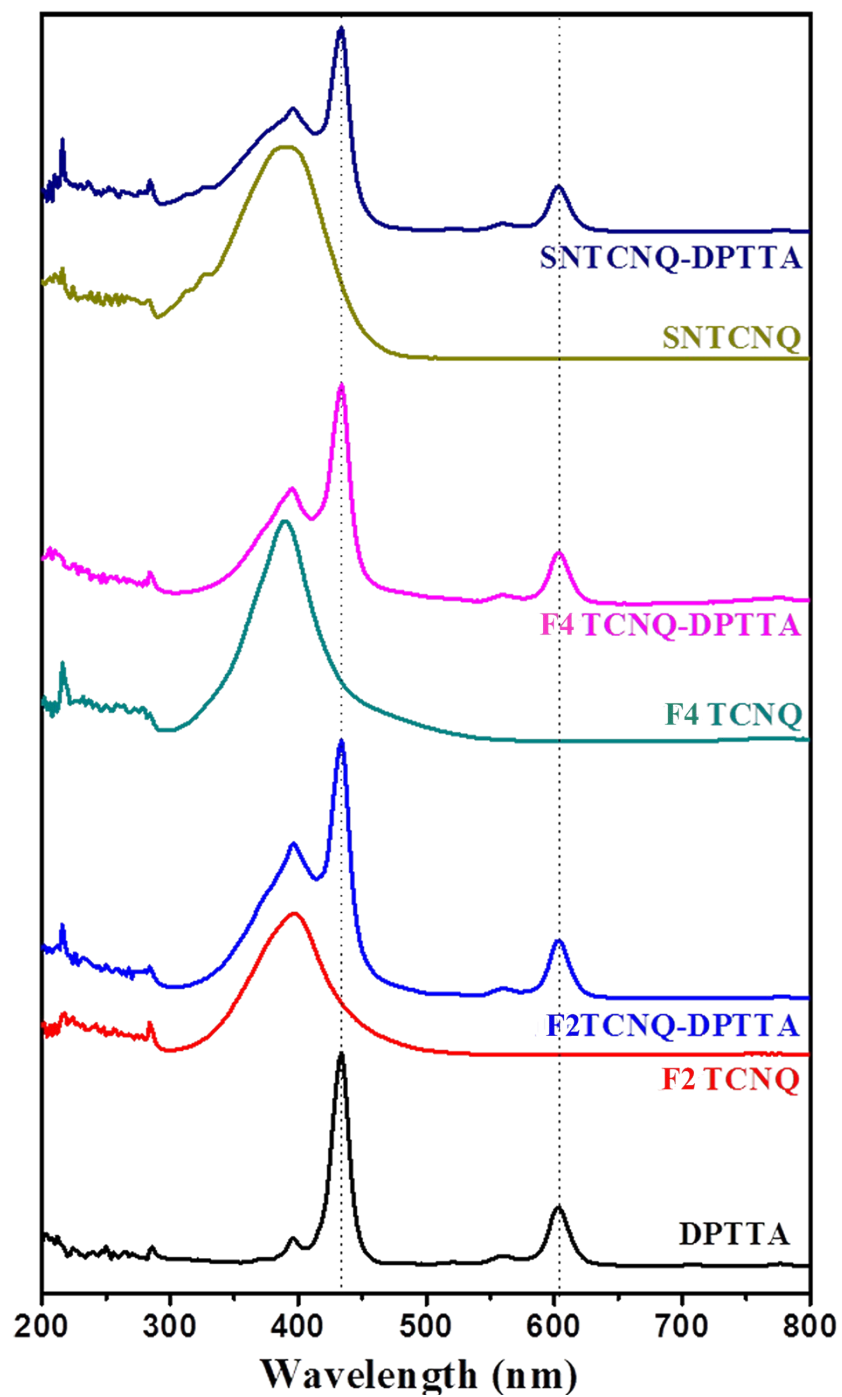


Fig. S1 UV-Vis spectrum of DPTTA-based CT complexes, together with corresponding pristine acceptors, and pristine DPTTA, measured in dilute chlorobenzene solution.

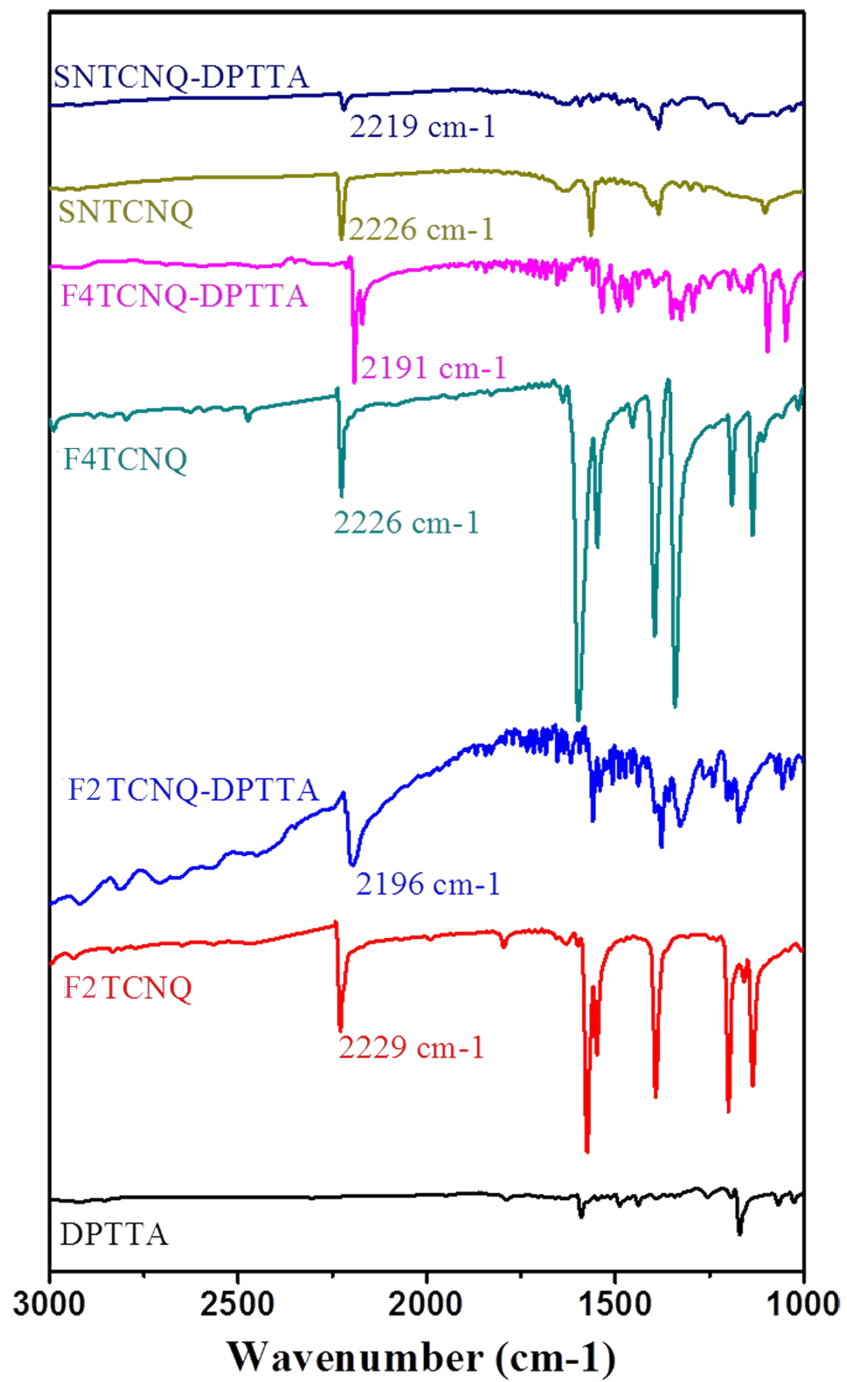


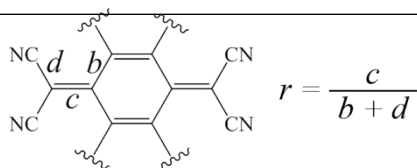
Fig. S2 FT-IR spectra of DPTTA-based CT complexes, together with corresponding pristine acceptors, and pristine DPTTA, measured in the dispersed KBr pellet.

Table S1. Crystal data and structure refinement of DPTTA-based complexes.

	F2TCNQ-DPTTA	F4TCNQ-DPTTA	SNTCNQ-DPTTA
Empirical formula	C ₄₆ H ₂₄ F ₂ N ₄ S ₄	C ₄₆ H ₂₂ F ₄ N ₄ S ₄	C ₄₆ H ₂₄ N ₆ S ₅
Formula weight	798.93	834.92	821.01
Temperature	100(2) K	100(2) K	173(2) K
Wavelength	0.71073 Å	0.71073 Å	0.71073 Å
Crystal system	Triclinic	Triclinic	Triclinic
space group	P -1	P -1	P -1
Unit cell dimensions	$a = 7.9146(16) \text{ \AA}; \alpha = 89.02(3)^\circ$ $b = 10.340(2) \text{ \AA}; \beta = 80.45(3)^\circ$ $c = 11.030(2) \text{ \AA}; \gamma = 82.36(3)^\circ$	$a = 7.9463(16) \text{ \AA}; \alpha = 88.15(3)^\circ$ $b = 10.099(2) \text{ \AA}; \beta = 81.09(3)^\circ$ $c = 11.251(2) \text{ \AA}; \gamma = 82.60(3)^\circ$	$a = 7.7712(16) \text{ \AA}; \alpha = 74.094(8)^\circ$ $b = 11.266(2) \text{ \AA}; \beta = 78.856(9)^\circ$ $c = 11.337(2) \text{ \AA}; \gamma = 80.050(9)^\circ$
Volume	882.2(3) Å ³	884.5(3) Å ³	928.9(3) Å ³
Z, Calculated density	1, 1.504 Mg/m ³	1, 1.567 Mg/m ³	1, 1.468 Mg/m ³
Absorption coefficient	0.323 mm ⁻¹	0.334 mm ⁻¹	0.358 mm ⁻¹
F(000)	410	426	422
Crystal size	0.45 x 0.17 x 0.05 mm	0.40 x 0.16 x 0.04 mm	0.35 x 0.21 x 0.21 mm
θ range for data collection	1.87 to 27.49 °	1.83 to 27.48 °	2.69 to 27.50 °
Limiting indices	-10 ≤ h ≤ 10; -13 ≤ k ≤ 13; -14 ≤ l ≤ 14	-10 ≤ h ≤ 10; -12 ≤ k ≤ 13; -14 ≤ l ≤ 14	-9 ≤ h ≤ 10; -14 ≤ k ≤ 14; -14 ≤ l ≤ 14
Reflections collected / unique	11582 / 4029 [R(int) = 0.0732]	12225 / 4042 [R(int) = 0.0871]	12106 / 4247 [R(int) = 0.0458]
Completeness to $\theta = 27.50$	99.7 %	99.5 %	99.4 %
Absorption correction	Semi-empirical from equivalents	Semi-empirical from equivalents	Semi-empirical from equivalents
Max. and min. transmission	1.0000 and 0.7160	1.0000 and 0.6057	1.0000 and 0.5622
Refinement method	Full-matrix least-squares on F ²	Full-matrix least-squares on F ²	Full-matrix least-squares on F ²
Data / restraints / parameters	4029 / 2 / 263	4042 / 0 / 262	4247 / 0 / 290
Goodness-of-fit on F ²	1.088	1.135	1.111
Final R indices [I > 2 σ (I)]	R1 = 0.0546 ; wR2 = 0.1251	R1 = 0.0821; wR2 = 0.1990	R1 = 0.0489; wR2 = 0.1133
R indices (all data)	R1 = 0.0691; wR2 = 0.1350	R1 = 0.0967; wR2 = 0.2124	R1 = 0.0520; wR2 = 0.1154
Largest diff. peak and hole	0.375 and -0.411 e.Å ⁻³	0.952 and -0.678 e.Å ⁻³	0.591 and -0.425 e.Å ⁻³

Table S2. CT characteristics of the complexes evaluated from changes in the bond lengths.

Complex	$r_{\delta=0}$ ^a	$r_{\delta=1}$ ^a	$r_{complex}$
F2TCNQ-DPTTA	0.477 ^b	0.496 ^e	0.485
F4TCNQ-DPTTA	0.476 ^c	0.500 ^e	0.500
SNTCNQ-DPTTA	0.470 ^d	-	0.475



^a $r_{\delta=0}$ and $r_{\delta=1}$ are the values for the neutral acceptor and for the fully ionized acceptor, respectively.

^bReference², ^cReference³, ^dReference⁴, ^eReference⁵.

Table S3. The first redox potentials ($E_{red} 1/V$) of pristine acceptors.

	F2TCNQ	F4TCNQ	SNTCNQ
$E_{red} 1/V$	0.41 ^a	0.60 ^a	0.12 ^b

^a Reference⁶, ^b Reference⁴.

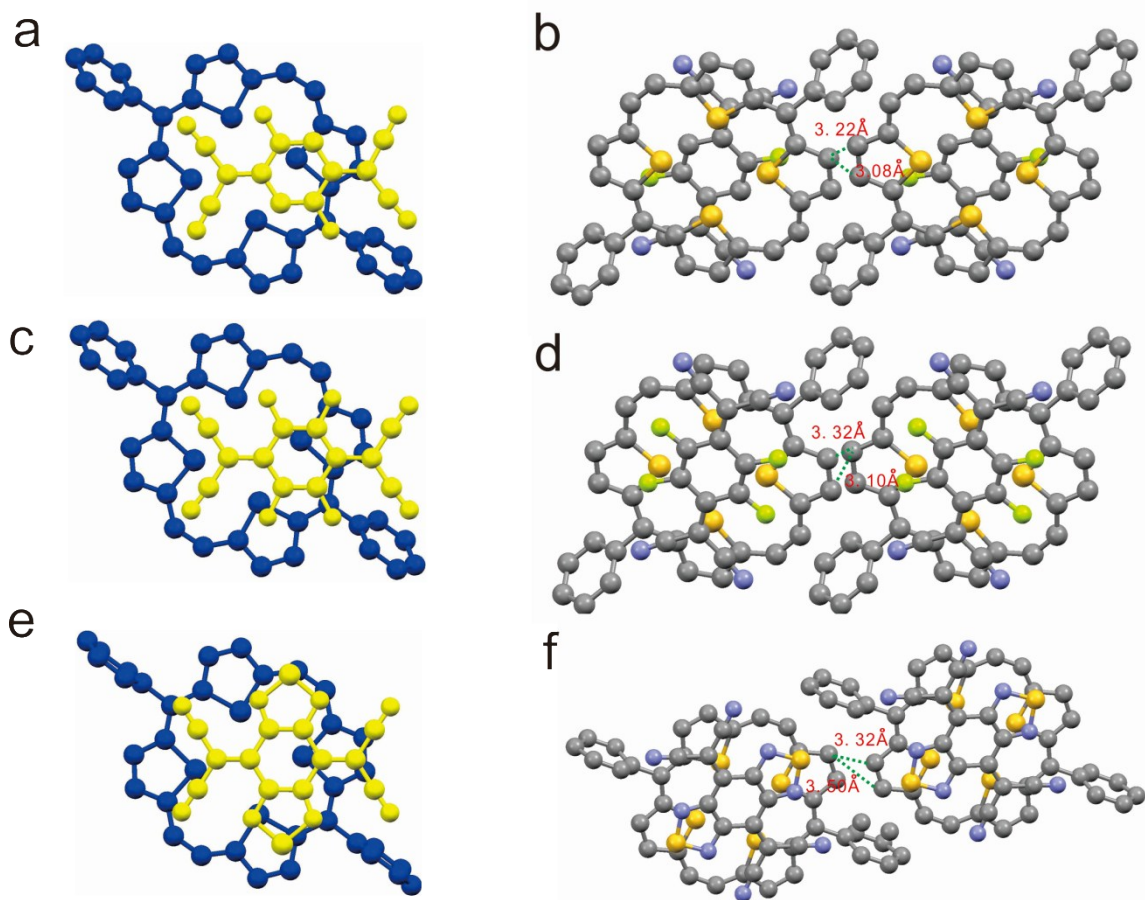


Fig. S3 Overlap patterns (view perpendicular to the DPTTA plane) and lateral π - π interactions between donor molecules in DPTTA-based complexes. a,b) for **F2TCNQ**-DPTTA; c,d) for **F4TCNQ**-DPTTA; e,f) for **SNTCNQ**-DPTTA (hydrogen atoms were omitted for clarity).

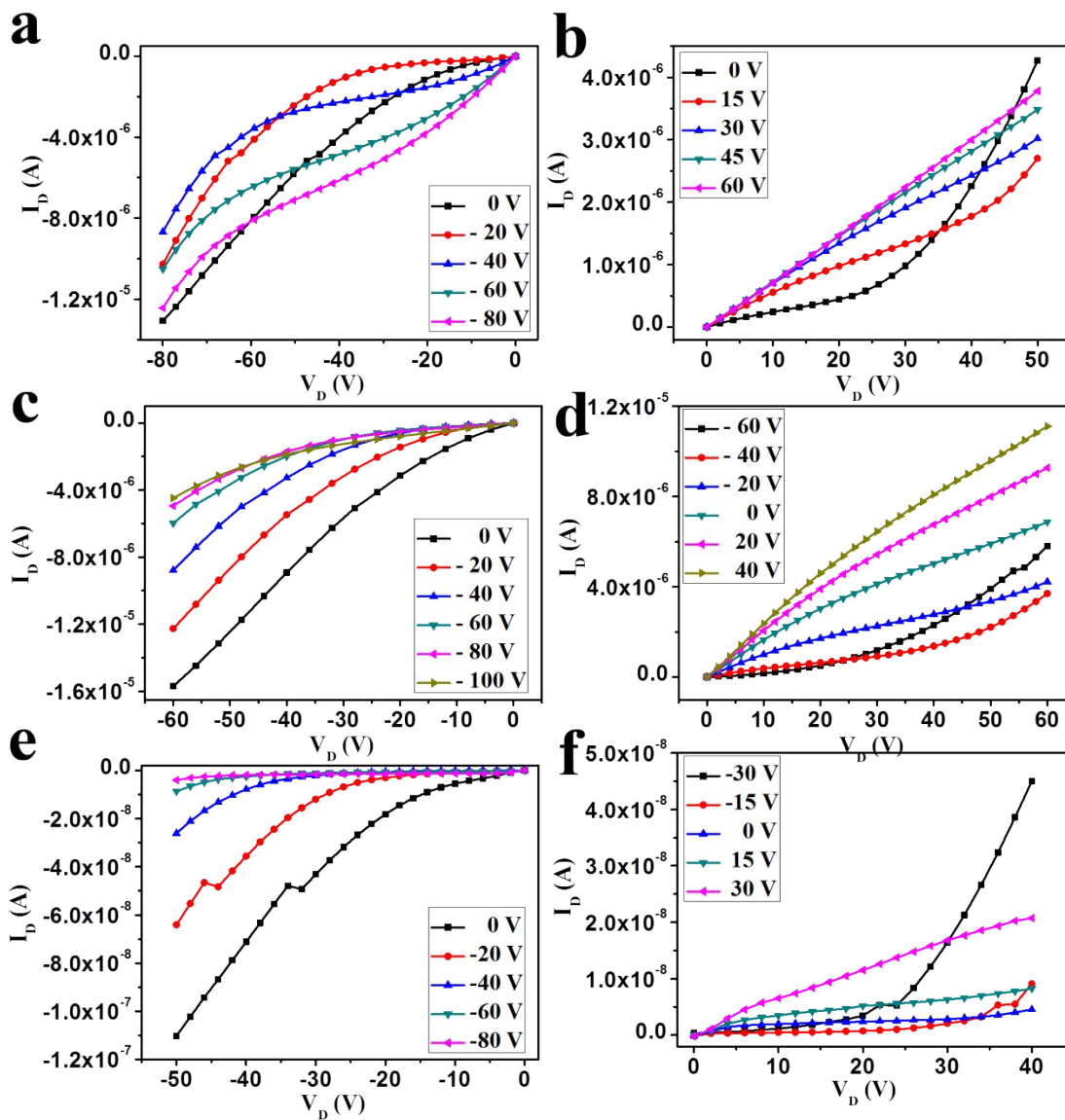


Fig. S4 Output curves of DPTTA-based complexes, corresponding to the presented transfer curves in the text. a,b) for F2TCNQ-DPTTA; c,d) for F4TCNQ-DPTTA; e,f) for SNTCNQ-DPTTA.

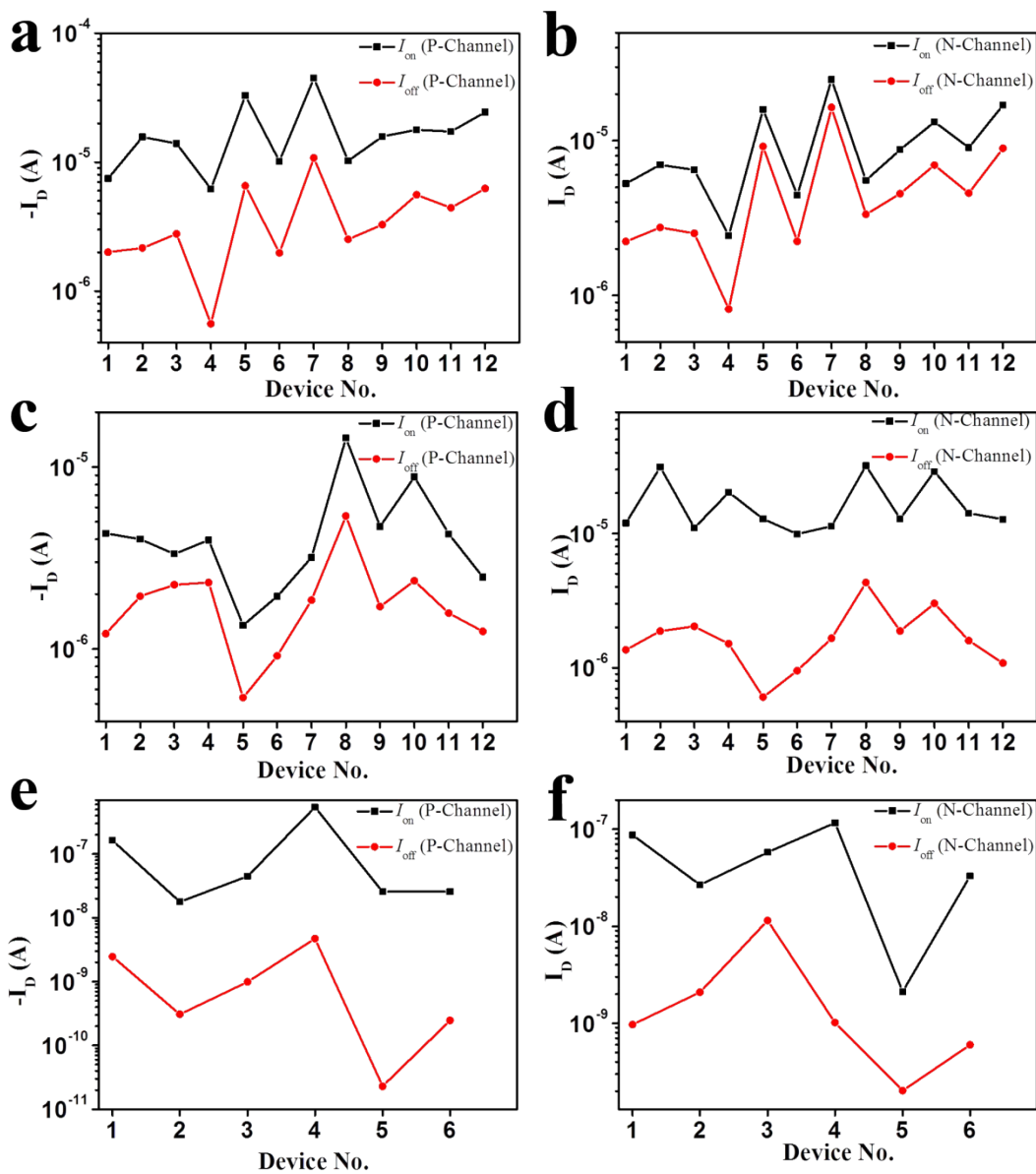


Fig. S5 The I_{on} and I_{off} distribution of DPTTA-based complex devices. The revealed low on/off ratios largely stem from the charge transfer-induced increases in off-currents a,b) for F2TCNQ-DPTTA; c,d) for F4TCNQ-DPTTA; e,f) for SNTCNQ-DPTTA.

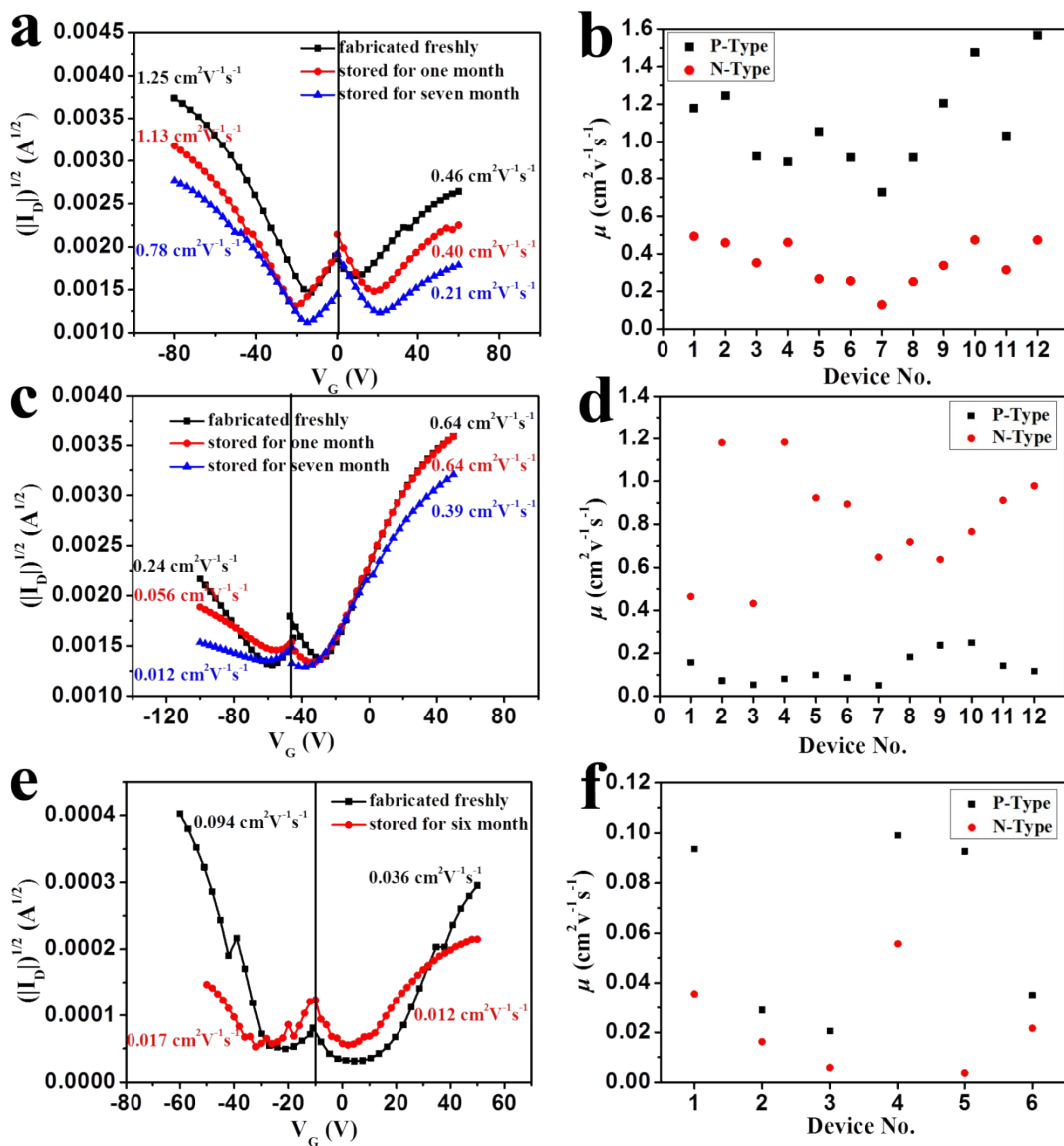
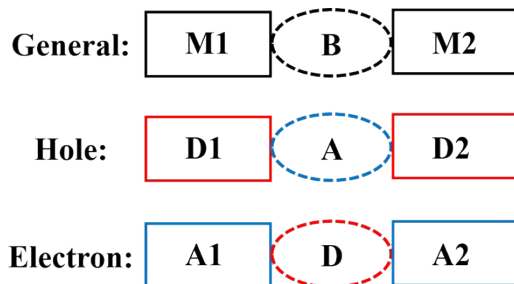


Fig. S6 The air-stability tests by contrast of typical transfer curve as well as mobility distribution of DPTTA-based complex devices. a,b) for F2TCNQ-DPTTA; c,d) for F4TCNQ-DPTTA; e,f) for SNTCNQ-DPTTA.

3. Theoretical Study and DFT Calculations

During the geometry optimizations of the crystal structures, the positions of the atoms in the unit cell were relaxed, while the cell parameters were kept fixed at the experimental values, the energy cutoff is set to 600 eV and a Monkhorst-Pack k-mesh of $6 \times 6 \times 6$ is used to obtain self-consistent charge density. The plane wave kinetic energy cutoff is set as 600 eV. The convergence criterion of the total energy is 10^{-5} eV in the self-consistent field iteration, and the maximum force allowed on each atom is 0.01 eV/Å.

In the super-exchange coupling calculation, A-D-A triad is used for electron and D-A-D triad is used for hole, as illustrated in Scheme S2. For D-A-D triad, donor 1 and donor 2 act as molecule 1 and molecule 2 in Formula (1) respectively and the in-between acceptor acts as the bridge. Correspondingly, for A-D-A triad, the in-between donor is the bridge.



Scheme S2. Schemes of DAD and ADA triads used for hole and electron super-exchange coupling calculations.

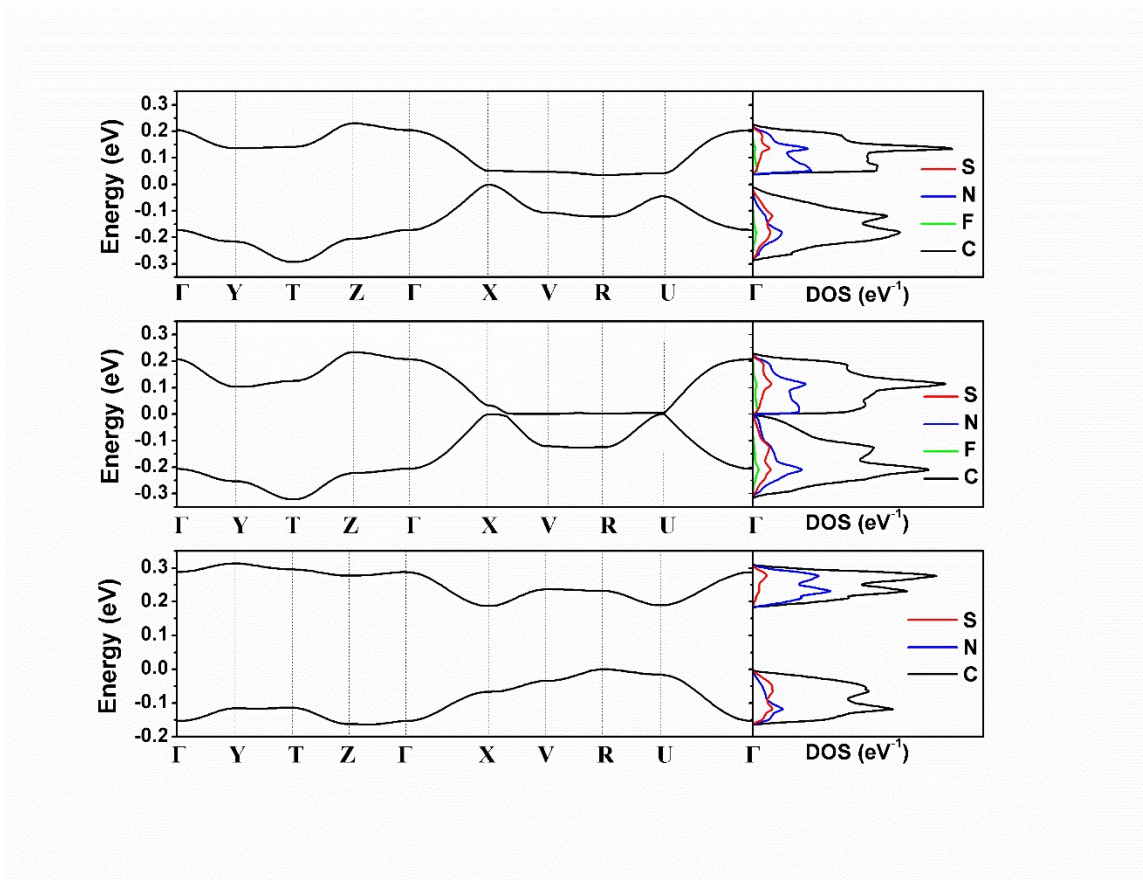


Fig. S7 Band structures of the 3,6-F2TCNQ-DPTTA (top panel), F4TCNQ-DPTTA (middle panel) and 2-SNTCNQ-DPTTA crystal (bottom panel). The reciprocal coordinates of high-symmetry points are $\Gamma=(0, 0, 0)$, $Y=(0, 0.5, 0)$, $T=(0, 0.5, 0.5)$, $Z=(0, 0, 0.5)$, $X=(0.5, 0, 0)$, $V=(0.5, 0.5, 0)$, $R=(0.5, 0.5, 0.5)$, $U=(0.5, 0, 0.5)$.

Table S4. Valence and conduction total bandwidths and related bandwidths along the D-A mixed stacking directions (in meV).

Crystal	VB W	CB W	VBW- stack	CBW- stack
2,5-F2TCNQ-DPTTA	329	224	225	205
3,6-F2TCNQ-DPTTA	298	206	172	195

F4TCNQ-DPTTA	316	239	206	172
1-SNTCNQ-DPTTA	165	127	88	102
2-SNTCNQ-DPTTA	165	127	87	102

4. References

- (1) Jiang, L.; Gao, J.; Wang, E.; Li, H.; Wang, Z.; Hu, W.; Jiang, L. *Adv. Mater.* **2008**, *20*, 2735.
- (2) Mitchell Wiygul, F.; Ferraris, J. P.; Emge, T. J.; Kistenmacher, T. J. *Mol. Cryst. Liq. Cryst.* **1981**, *78*, 279.
- (3) Emge, T. J.; Maxfield, M.; Cowan, D. O.; Kistenmacher, T. J. *Mol. Cryst. Liq. Cryst.* **1981**, *65*, 161.
- (4) Suzuki, T.; Yamashita, Y.; Fukushima, T.; Miyashi, T. *Mol. Cryst. Liq. Cryst.* **1997**, *296*, 165.
- (5) Jose-Larong, J. F. F.; Takahashi, Y.; Inabe, T. *Struct. Chem.* **2013**, *24*, 113.
- (6) Yoshida, Y.; Shimizu, Y.; Yajima, T.; Maruta, G.; Takeda, S.; Nakano, Y.; Hiramatsu, T.; Kageyama, H.; Yamochi, H.; Saito, G. *Chem. Eur. J.* **2013**, *19*, 12313.